ADVANCES IN ATMOSPHERIC SCIENCES, VOL. 23, NO. 4, 2006, 504–512

Shearing Wind Helicity and Thermal Wind Helicity

HAN Ying (韩 瑛), WU Rongsheng* (伍荣生), and FANG Juan (方 娟)

The Key Laboratory of Mesoscale Severe Weather, Nanjing University, Nanjing 210093

(Received 24 June 2005; revised 12 December 2005)

ABSTRACT

Helicity is defined as $H = \boldsymbol{V} \cdot \boldsymbol{\omega}$, where $\boldsymbol{V}$ and $\boldsymbol{\omega}$ are the velocity and vorticity vectors, respectively. Many works have pointed out that the larger the helicity is, the longer the life cycle of the weather system is. However, the direct relationship of the helicity to the evolution of the weather system is not quite clear. In this paper, the concept of helicity is generalized as shearing wind helicity (SWH). Dynamically, it is found that the average SWH is directly related to the increase of the average cyclonic rotation of the weather system. Physically, it is also pointed out that the SWH, as a matter of fact, is the sum of the torsion terms and the divergence term in the vorticity equation. Thermal wind helicity (TWH), as a derivative of SWH, is also discussed here because it links the temperature field and the vertical wind field. These two quantities may be effective for diagnosing a weather system. This paper applies these two quantities in cylindrical coordinates to study the development of Hurricane Andrew to validate their practical use. Through analyzing the hurricane, it is found that TWH can well describe the characteristics of the hurricane such as the strong convection and release of latent heat. SWH is not only a good quantity for diagnosing the weather system, but also an effective one for diagnosing the development of the hurricane.

Key words: helicity, shearing wind helicity, thermal wind helicity, hurricane, SWH, TWH

doi: 10.1007/s00376-006-0504-5

1. Introduction

Based on the definition of helicity and potential vorticity, Wu and Tan (1989) proposed the conception of the generalized vorticity (GV), which has the following form:

$$\boldsymbol{\zeta}_{\mathrm{G}} = \boldsymbol{\psi} \cdot \boldsymbol{\omega}_a \, , \tag{1}$$

where $\boldsymbol{\psi}$ is an arbitrary vector and $\boldsymbol{\omega}_a$ is the vorticity, and the balance of $\boldsymbol{\zeta}_{\mathrm{G}}$ was discussed in detail in their work. If $\boldsymbol{\psi}$ is taken as the gradient of the potential temperature ($\nabla\theta$), the vorticity ($\boldsymbol{\omega}_a$), and the velocity ($\boldsymbol{V}$), then the $\boldsymbol{\zeta}_{\mathrm{G}}$ corresponds to potential vorticity (Hoskins et al, 1985), enstrophy (Wu, 1984), and helicity (Tan and Wu, 1994), respectively. Thus these quantities can be considered as a type of $\boldsymbol{\zeta}_{\mathrm{G}}$, however they each have their own distinctive features. For instance, the potential vorticity combines the vorticity field and potential temperature field together. Enstrophy describes the intensity of the air rotation. Helicity is the scalar product of the vorticity and velocity vectors. It measures the strength of the rotation in the direction of the air motion or that of the air motion in the direction of rotation.

Due to its clear physical meaning, helicity has important applications in meteorology. For example, many meteorologists use helicity to study the properties of severe weather systems such as tornadoes, hurricanes, squall lines and so on (Etling, 1985; Brown, 1980; Lilly, 1986, 1990; Chen and Tan, 1999; Xu and Wu, 2003). These researchers have pointed out that if the direction of rotation is parallel to the motion, i.e. the helicity is large, the effect of advection is cancelled by stretching and tilting, so the weather system can last a long time. However, there is no direct relationship between the helicity and the intensity variation of the weather system theoretically except in a very special case, which will be demonstrated in the appendix. In this work, a new quantity is introduced by taking $\boldsymbol{\psi}$ in Eq. (1) as the vertical shear of the wind, viz., $\partial\boldsymbol{V}/\partial z$. In this case, we name $\boldsymbol{\zeta}_G$ as the shearing wind helicity (SWH) since it becomes the physical relation between the vorticity and the shearing wind. In fact, for the large-scale motion, $\partial\boldsymbol{V}/\partial z$ can be approximated by the thermal wind, and thus SWH depicts the strength of rotation in the direction of the thermal wind or that of the thermal wind in the direction of rotation. In this situation, SWH is called the thermal wind helicity (TWH).

In this paper, the advantages and disadvantages of the helicity, SWH and TWH are discussed in section 2. New forms of TWH and SWH applied to a hurricane

*E-mail: rwu@nju.edu.cn

are defined in the third section. The distribution characteristics of TWH and SWH in a hurricane are presented in section 4. A case study on the development of a hurricane with these new quantities is presented in section 5. Finally, concluding remarks are given in the last section.

2. Dynamic features of helicity, shearing wind helicity and thermal wind helicity

2.1 *Helicity*

According to the definition of helicity, it is expressed as

$$H = \boldsymbol{V} \cdot \boldsymbol{\omega} \,, \tag{2}$$

where $\boldsymbol{V}$ and $\boldsymbol{\omega}$ are the velocity and vorticity vectors respectively, viz.

$$\boldsymbol{V} = u\boldsymbol{i} + v\boldsymbol{j} + w\boldsymbol{k} \,, \tag{3}$$

$$\boldsymbol{\omega} = \nabla \times \boldsymbol{V} = \left(\frac{\partial w}{\partial y} - \frac{\partial v}{\partial z}\right)\boldsymbol{i} + \left(\frac{\partial u}{\partial z} - \frac{\partial w}{\partial x}\right)\boldsymbol{j} + \left(\frac{\partial v}{\partial x} - \frac{\partial u}{\partial y}\right)\boldsymbol{k} = \xi\boldsymbol{i} + \eta\boldsymbol{j} + \zeta\boldsymbol{k} \,. \tag{4}$$

where ξ, η, and ζ are the x, y, and the vertical components of the vorticity, respectively.

If the effect of the earth's rotation is taken into account, then the absolute vorticity is written as

$$\boldsymbol{\omega}_a = \nabla \times \boldsymbol{V} + 2\boldsymbol{\Omega} = \xi\boldsymbol{i} + (\eta\boldsymbol{j} + \overline{f}) + (\zeta + f)\boldsymbol{k} \,, \tag{5}$$

where $f = 2\Omega\sin\phi$ and $\overline{f} = 2\Omega\cos\varphi$, and where the latter is usually smaller and is ignored hereafter. Ω, ϕ, and φ are the angular velocity of the earth, latitude, and longitude, respectively. Substituting $\boldsymbol{\omega}_a$ into Eq. (2) gives

$$H = u\left(\frac{\partial w}{\partial y} - \frac{\partial v}{\partial z}\right) + v\left(\frac{\partial u}{\partial z} - \frac{\partial w}{\partial x}\right) + w\left(\frac{\partial v}{\partial x} - \frac{\partial u}{\partial y} + f\right) \,. \tag{6}$$

Since $\boldsymbol{V}$ and $\boldsymbol{\omega}$ are vectors, then the sign of helicity is dependent on the relative direction of both vectors. For example, if the two vectors are in the same direction, H is positive. H is negative when the vectors are in opposite directions. However, positive or negative helicity does not imply the strengthening or weakening of the weather system. In general, there is no direct relationship between the helicity and the intensity change of the weather system, except in a very special case, which is demonstrated in the appendix.

2.2 *Shearing wind helicity*

2.2.1 *Definition of shearing wind helicity*

The situation discussed above will be changed if we generalize the conception of helicity to the SWH, in which the shearing wind vector is used instead of the wind vector in the definition of helicity. The SWH is defined as

$$H_s = \boldsymbol{\omega}_a \cdot \frac{\partial \boldsymbol{V}}{\partial z} \,. \tag{7}$$

Comparing Eqs. (2) and (7), we can find different dynamic features and the advantage of the SWH. Since the dimension of the vorticity is

$$[\boldsymbol{\omega}_a] = \frac{1}{T} \,, \tag{8}$$

the dimension of the SWH is

$$[H_s] = \frac{[\boldsymbol{V}]}{L} \cdot \frac{1}{T} = \frac{[\boldsymbol{\omega}_a]}{T} \,. \tag{9}$$

where T is the time scale, L is the length scale, and the dimension of the velocity $[\boldsymbol{V}] = L/T$. This is equivalent to the dimension of $\partial\boldsymbol{\omega}_a/\partial t$. Thus it means the SWH is physically associated with the change of vorticity with time. This point can be further demonstrated as follows.

Expanding the expression in terms of Eqs. (2), (3) and (4) gives

$$H_s = \left(\frac{\partial w}{\partial y} - \frac{\partial v}{\partial z}\right)\frac{\partial u}{\partial z} + \left(\frac{\partial u}{\partial z} - \frac{\partial w}{\partial x}\right)\frac{\partial v}{\partial z} + \left(\frac{\partial v}{\partial x} - \frac{\partial u}{\partial y} + f\right)\frac{\partial w}{\partial z} \,. \tag{10}$$

After manipulation, SWH can be expressed as

$$H_s = \frac{\partial w}{\partial y}\frac{\partial u}{\partial z} - \frac{\partial w}{\partial x}\frac{\partial v}{\partial z} + \left(\frac{\partial v}{\partial x} - \frac{\partial u}{\partial y} + f\right)\frac{\partial w}{\partial x} \,. \tag{11}$$

The first two terms on the right of Eq. (11) are the torsion terms, and the third is the divergence term of the physical vorticity equation. In other words, these two terms are combined together and form concisely a new quantity as SWH. To our knowledge, this has not been discussed in the literature before.

From Eq. (7), it is plausible that the vorticity $\boldsymbol{\omega}_a$ will be twisted due to the vertical shearing of the wind, which will then cause the change of strength of the vertical component of the vorticity (see Fig. 1). Thus the magnitude of SWH has the physical meaning of the change in vertical vorticity. This provides a valuable factor for diagnosing the development of the system.

We can also illustrate the properties of the SWH from a dynamic point of view. For an incompressible fluid, the equation of motion can be expressed as

$$\frac{\partial \boldsymbol{V}}{\partial t} + \boldsymbol{V} \cdot \nabla\boldsymbol{V} = -\frac{1}{\rho}\nabla p - 2\boldsymbol{\Omega} \times \boldsymbol{V} + \boldsymbol{g} \,, \tag{12}$$

and the continuity equation is

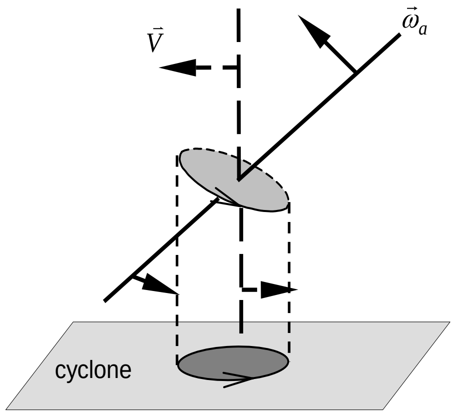

Fig. 1. A schematic illustration of the physical meaning of SWH.

$$\frac{\partial u}{\partial x} + \frac{\partial v}{\partial y} + \frac{\partial w}{\partial z} = 0 , \tag{13}$$

where $\boldsymbol{g}, \rho$, and p are the gravity, density and pressure of the atmosphere, respectively. From these equations, we can obtain the vertical component of the vorticity equation as follows:

$$\frac{d}{dt}(\zeta+f) = -(\zeta+f)\left(\frac{\partial u}{\partial x}+\frac{\partial v}{\partial y}\right) - \left(\frac{\partial w}{\partial x}\frac{\partial v}{\partial z} - \frac{\partial w}{\partial y}\frac{\partial u}{\partial z}\right) + N_z , \tag{14}$$

where

$$N_z = \frac{1}{\rho^2}\left(\frac{\partial \rho}{\partial x}\frac{\partial p}{\partial y} - \frac{\partial \rho}{\partial y}\frac{\partial p}{\partial x}\right)$$

is the solenoid term in the vertical direction. Actually, if the solenoid term is ignored Eq. (14) can be rewritten as:

$$\frac{d}{dt}(\zeta+f) \approx \frac{\partial w}{\partial y}\frac{\partial u}{\partial z} - \frac{\partial w}{\partial x}\frac{\partial v}{\partial z} + (\zeta+f)\frac{\partial w}{\partial z} = H_s . \tag{15}$$

Thus, the SWH is closely related with the individual change of vorticity of the particle. This implies that the SWH has the potential ability to forecast. Since

$$\frac{d}{dt}(\zeta+f) = \frac{\partial}{\partial t}(\zeta+f) + \nabla\cdot[\boldsymbol{V}(\zeta+f)] - (\zeta+f)\nabla\cdot\boldsymbol{V} , \tag{16}$$

the last term on the right side vanishes under the condition of non-divergence. Consequently, Eq. (15) can be further simplified as

$$\frac{d}{dt}(\zeta+f) = \frac{\partial}{\partial t}(\zeta+f) + \nabla\cdot\boldsymbol{V}(\zeta+f) . \tag{17}$$

Suppose there is a system with volume τ. Integrating Eq. (15) by means of Eq. (17) yields

$$\begin{aligned}&\iiint_\tau \frac{\partial}{\partial t}(\zeta+f)d\tau + \iiint_\tau \nabla\cdot[\boldsymbol{V}(\zeta+f)]d\tau \\ &= \iiint_\tau \frac{\partial}{\partial t}(\zeta+f)d\tau + \iint_\sigma \boldsymbol{n}\cdot\boldsymbol{V}(\zeta+f)d\sigma \\ &= \iiint_\tau H_s d\tau ,\end{aligned} \tag{18}$$

where σ is the surface of the system and $\boldsymbol{n}$ is the outward unit normal of the surface. Alternatively, Eq. (18) can be rewritten as

$$\frac{\partial}{\partial t}\overline{\zeta} = \overline{H}_s + F_n , \tag{19}$$

where $\overline{\zeta}$ and $\overline{H}_s$ are the volume averaged vorticity and SWH, respectively. Namely

$$\boldsymbol{\zeta} = \frac{\iiint_\tau (\zeta+f)d\tau}{\iiint_\tau d\tau} , \tag{20}$$

$$\overline{H}_s = \frac{\iiint_\tau H_s d\tau}{\iiint_\tau d\tau} , \tag{21}$$

F_n is the flux through the boundary of the volume. Hence, for an isolated system, Eq. (19) can be simplified as

$$\frac{\partial}{\partial t}\overline{\zeta} = \overline{H}_s . \tag{22}$$

This indicates that the SWH is the producing term of the vertical component of vorticity. Thus, it is a valuable and useful variable for diagnosing the development of a system.

2.2.2 *Generalization of shearing wind helicity*

Similar to the treatment of Eq. (14), the x and y components of the vorticity equation can be expressed as:

$$\frac{d\xi}{dt} = \boldsymbol{\omega}_a \cdot \frac{\partial \boldsymbol{V}}{\partial x} + f\eta + N_x \tag{23}$$

$$\frac{d\eta}{dt} = \boldsymbol{\omega}_a \cdot \frac{\partial \boldsymbol{V}}{\partial y} - f\xi + N_y \tag{24}$$

where

$$N_x = \frac{1}{\rho^2}\left(\frac{\partial \rho}{\partial y}\frac{\partial p}{\partial z} - \frac{\partial \rho}{\partial z}\frac{\partial p}{\partial y}\right)$$

and

$$N_y = \frac{1}{\rho^2}\left(\frac{\partial \rho}{\partial z}\frac{\partial p}{\partial x} - \frac{\partial \rho}{\partial x}\frac{\partial p}{\partial z}\right)$$

are the solenoid components in the x and y direction. Accordingly, we can define the new quantity SWH with the symbol H_{si} as

$$H_{si} = \boldsymbol{\omega}_a \cdot \frac{\partial \boldsymbol{V}}{\partial x_i} , \tag{25}$$

where $i = 1, 2, 3$ represent the x, y, and z direction, respectively, and where H_{si} denotes the helicity, which is formed by the shearing wind in the x_i direction. Moreover, H_{si} is the projection of the torsion term in the x_i direction, and thus it can induce the variation of the vorticity in the x_i direction. Using Eq. (25), Eqs. (23) and (24) can be rearranged as

$$\begin{cases} \dfrac{\partial \xi}{\partial t} = H_{s1} + f\eta + N_x \\ \dfrac{\partial \eta}{\partial t} = H_{s2} - f\xi + N_y . \end{cases} \tag{26}$$

From these results we can conclude that for an incompressible fluid, the new SWH is closely related to the change of vorticity in the case that the baroclinic effect is not significant. Thus, the evolution of some vertical circulations such as the sea breeze and mountain-valley circulation may be diagnosed with the help of the SWH, H_{s1} and H_{s2}.

2.3 *Thermal wind helicity*

The situation discussed above just shows the dynamic features of SWH. However TWH is used to describe the thermal features of SWH. For the synoptic-scale motions, horizontal wind can be replaced by geostrophic wind with good accuracy. H_s can be expressed approximately as follows when the horizontal part of shearing wind is substituted with geostrophic wind. Thus, the thermal wind helicity is generated, which depicts the strength of rotation in the direction of the thermal wind or that of the thermal wind in the direction of rotation.

$$\begin{aligned} H_s &\approx \boldsymbol{\omega}_{gh} \cdot \frac{\partial \boldsymbol{V}_g}{\partial z} + (\zeta + f)\frac{\partial w}{\partial z} \\ &= \boldsymbol{\omega}_{gh} \cdot \boldsymbol{V}_T + (\zeta + f)\frac{\partial w}{\partial z} , \end{aligned} \tag{27}$$

where $\boldsymbol{\omega}_{gh}$ is the horizontal geo-vorticity, and where

$$\boldsymbol{V}_T = \frac{\partial u_g}{\partial z}\boldsymbol{i} + \frac{\partial v_g}{\partial z}\boldsymbol{j}$$

is the thermal wind, viz.

$$\frac{\partial u_g}{\partial z} = -\frac{g}{f}\frac{\partial}{\partial y}\ln T , \quad \frac{\partial v_g}{\partial z} = \frac{g}{f}\frac{\partial}{\partial x}\ln T . \tag{28}$$

Substituting Eq. (28) into Eq. (27) gives

$$\begin{aligned} H_s &\approx -\frac{g}{f}(\nabla \ln T \cdot \nabla w) + (\zeta + f)\frac{\partial w}{\partial z} \\ &= H_1 + H_2 , \end{aligned} \tag{29}$$

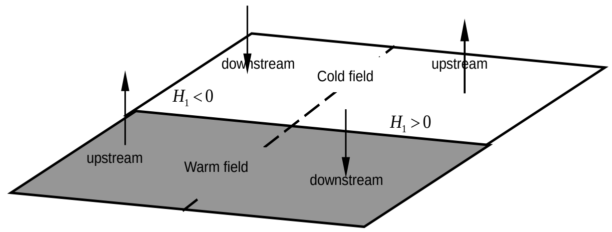

Fig. 2. A schematic illustration of the physical meaning of TWH.

where

$$H_1 = -\frac{g}{f}(\nabla \ln T \cdot \nabla w) , \tag{30}$$

$$H_2 = (\zeta + f)\frac{\partial w}{\partial z} . \tag{31}$$

H_1 is defined as the thermal wind helicity (TWH). Since $\boldsymbol{\psi}$ is an arbitrary vector $\boldsymbol{\omega}_a$ and $\boldsymbol{\psi}$ and are not independent of each other in the generalized vorticity, $\boldsymbol{\zeta}_G = \boldsymbol{\psi} \cdot \boldsymbol{\omega}_a$. We can take $\boldsymbol{\psi}$ as $\partial \boldsymbol{V}_g/\partial z$, and $\boldsymbol{\omega}_a$ is replaced with $\boldsymbol{\omega}_{ga}$, and so we can also get H_1. Clearly the TWH is another kind of generalized vorticity. This quantity shows the relationship between the vertical velocity field and temperature field, which has an advantage as a potential vorticity. If there is upstream flow in the warm field and downstream flow in the cold field, then from Eq. (30) we can obtain $H_1 < 0$; on the contrary, if there is downstream flow in the warm field and upstream flow in the cold field, then $H_1 > 0$. That means we can estimate the direction of motion only from an ichnography of the TWH field. The thermal field and dynamic field are connected by TWH, which shows the thermal effect of SWH. The schematic diagram is shown in Fig. 2.

A hurricane is an isolated system with little flux across its boundaries. By means of the continuity equation (13), H_2 can be written as

$$H_2 = (\zeta + f)\frac{\partial w}{\partial z} = -(\zeta + f)\left(\frac{\partial u}{\partial x} + \frac{\partial v}{\partial y}\right) . \tag{32}$$

Clearly H_2 is approximated by the divergence term of the vorticity equation.

From Eq. (22), we obtain:

$$\frac{\partial}{\partial t}\overline{\zeta} = \overline{H}_s = \overline{H}_1 + \overline{H}_2 , \tag{33}$$

where $\overline{H}_1$ and $\overline{H}_2$ are the volume-averaged TWH and divergence term, respectively, viz.

$$\overline{H}_1 = \frac{\iiint\limits_\tau H_1 d\tau}{\iiint\limits_\tau d\tau} , \tag{34}$$

$$\overline{H}_2 = \frac{\iiint\limits_\tau H_2 d\tau}{\iiint\limits_\tau d\tau} . \tag{35}$$

3. TWH and SWH in a hurricane

Maximum tangential wind speeds in a hurricane range typically from 50 to 100 m s^{-1}. For such high velocities and relatively small scales, the centrifugal force term cannot be neglected compared to the Coriolis force. Thus, the tangential velocity in a steady-state hurricane is in gradient wind balance with the radial pressure gradient force. An expression for the thermal wind in a hurricane can be easily derived starting from the gradient wind balance in cylindrical coordinates (r, θ, z) (Holton, 2004), which can be written as

$$f v_\theta + \frac{v_\theta^2}{r} = \frac{1}{\rho}\frac{\partial p}{\partial r}\,, \tag{36}$$

$$f v_{\rm r} + \frac{v_\theta v_{\rm r}}{r} = -\frac{1}{\rho r}\frac{\partial p}{\partial \theta}\,, \tag{37}$$

where r is the radial distance from the axis of the storm (positive outward), v_θ is the tangential velocity (positive for anticlockwise flow), and $v_{\rm r}$ is the radial velocity (positive outward). Taking $\partial(36)/\partial z$ and $\partial(37)/\partial z$ gives

$$\frac{\partial v_\theta}{\partial z} = \frac{g\dfrac{\partial \ln T}{\partial r}}{f + \dfrac{2v_\theta}{r}}\,, \tag{38}$$

$$\frac{\partial v_{\rm r}}{\partial z} = \frac{-g\dfrac{\partial \ln T}{r\partial \theta} - \dfrac{v_{\rm r}}{r}\dfrac{\partial v_\theta}{\partial z}}{f + \dfrac{v_\theta}{r}}\,. \tag{39}$$

In a hurricane, the value of tangential velocity is much larger than the radial velocity, and

$$\frac{v_\theta}{r} \sim (1\times10^{-3} - 5\times10^{-4})\,,$$

so

$$\left(f + \frac{v_\theta}{r}\right) \sim \frac{v_\theta}{r}\,.$$

Thus Eqs. (38) and (39) can be rewritten as

$$\frac{\partial v_\theta}{\partial z} \approx \frac{1}{2}\frac{g\dfrac{\partial \ln T}{\partial r}}{\dfrac{v_\theta}{r}}\,, \tag{40}$$

$$\frac{\partial v_{\rm r}}{\partial z} \approx \frac{-g\dfrac{\partial \ln T}{r\partial \theta}}{\dfrac{v_\theta}{r}}\,, \tag{41}$$

Substituting Eqs. (40) and (41) into Eq. (11) will give

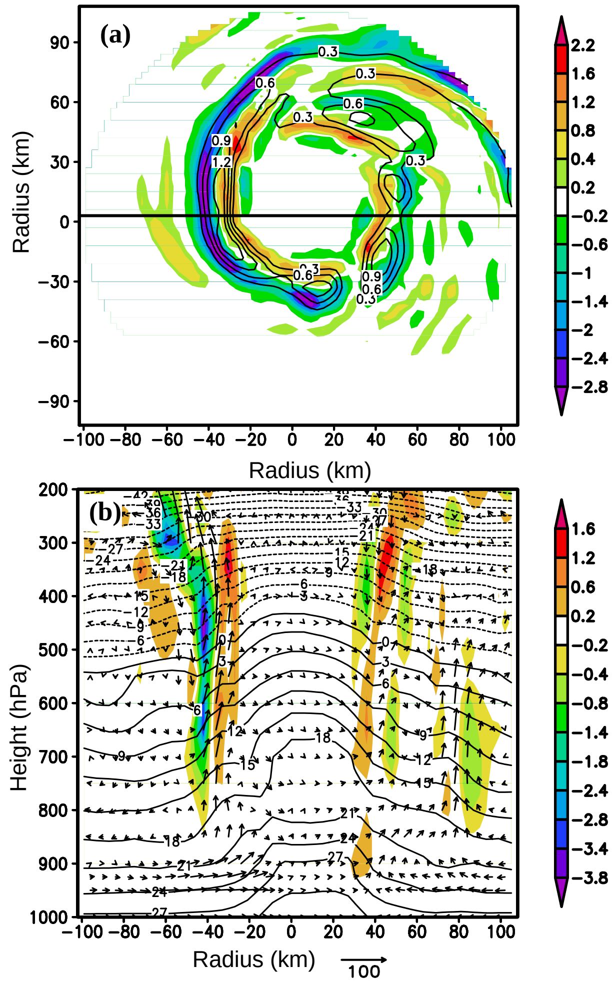

Fig. 3. TWH of Hurricane Andrew at 0900 UTC 23 August 1992. (a) TWH (shading, 0.0001 s^{-2}) and cloud water mixing (contours, g kg $^{-1}$) at 4000 hPa. (b) Vertical cross section of TWH (shading, 0.0001 s^{-2}), temperature (contours, °C) and $u-w$ vectors along the heavy line in (a).

$$\begin{aligned} H_s &= \left(\frac{1}{r}\frac{\partial w}{\partial \theta} - \frac{\partial v_\theta}{\partial z}\right)\frac{\partial v_{\rm r}}{\partial z} + \left(\frac{\partial v_{\rm r}}{\partial z} - \frac{\partial w}{\partial r}\right)\frac{\partial v_\theta}{\partial z} + \\ &\quad (\zeta + f)\frac{\partial w}{\partial z} \\ &\approx -\frac{g}{\dfrac{v_\theta}{r}}\left[\frac{\partial w}{r\partial \theta}\frac{\partial \ln T}{r\partial \theta} + \frac{1}{2}\frac{\partial \ln T}{\partial r}\left(\frac{\partial w}{\partial r} + \frac{v_{\rm r}}{v_\theta}\frac{\partial w}{r\partial \theta}\right)\right] + \\ &\quad (\zeta + f)\frac{\partial w}{\partial z} \\ &\approx -\frac{g}{\dfrac{v_\theta}{r}}\left[\frac{\partial w}{r\partial \theta}\frac{\partial \ln T}{r\partial \theta} + \frac{1}{2}\frac{\partial \ln T}{\partial r}\left(\frac{\partial w}{\partial r}\right)\right] + \\ &\quad (\zeta + f)\frac{\partial w}{\partial z} = H_1 + H_2\,, \end{aligned} \tag{42}$$

where

$$H_1 = -\frac{g}{\frac{v_\theta}{r}}\left[\frac{\partial w}{r\partial\theta}\frac{\partial \ln T}{r\partial\theta}+\frac{1}{2}\frac{\partial \ln T}{\partial r}\left(\frac{\partial w}{\partial r}\right)\right] , \quad (43)$$

$$H_2 = (\zeta + f)\frac{\partial w}{\partial z} . \quad (44)$$

Eq. (43) is the TWH in a hurricane, which is composed of two components, the radial part (H_{1r}) and the tangential part (H_{1t}):

$$H_{1r} = -\frac{g}{\frac{v_\theta}{r}}\left(\frac{\partial w}{r\partial\theta}\frac{\partial \ln T}{r\partial\theta}\right) , \quad (45)$$

$$H_{1t} = -\frac{g}{\frac{v_\theta}{r}}\left[\frac{1}{2}\frac{\partial \ln T}{\partial r}\left(\frac{\partial w}{\partial r}\right)\right] . \quad (46)$$

Since a hurricane is an approximate axisymmetric weather system, from Eq. (45), the value of H_{1r} is small. From Eq. (46), it can be inferred that H_{1t} describes the temperature and vertical velocity change in the radial direction. From observation, we know that hurricanes are warm core systems, thus $\partial T/\partial r < 0$; the intense convection and strong winds are in the eyewall, so from the eye to eyewall $\partial w/\partial r > 0$, thus $H_{1t} > 0$; from the eyewall to the outside $\partial w/\partial r < 0$, $H_{1t} < 0$. We can draw the image of TWH distributed in a hurricane, divided by the eyewall: inside is the positive TWH region, and outside is the negative TWH region.

4. The Distribution Characteristics of TWH and SWH in Hurricane Andrew

In this section, the general features of TWH and SWH are presented in Hurricane Andrew.

Hurricane Andrew (1992) was one of the most severe disasters in the history of the United States. Its simulation has been made and verified by Liu et al. (1997, 1999). Their model output of the finest mesh domain with a grid size of 6 km, and which was generated every 3 hours, is used in this study.

Equation (43) is used to calculate TWH of Hurricane Andrew at the mature stage (at 0900 UTC 23 August 1992). The distribution of TWH and cloud water mixing at 400 hPa are shown in Fig. 3a. We find that the cloud water is well matched with TWH, and the center of the cloud water lies in the interface between the positive and negative TWH zones. Figure 3b shows the vertical cross section of TWH, temperature and $\boldsymbol{u}-\boldsymbol{w}$ vectors along the heavy line in Fig. 3a. The eyewall, which corresponds to the region of intense convection and strong winds of the hurricane, is the division between positive and negative TWH. The contribution of TWH is mainly in the layer between 800 and 200 hPa.

Based on the above statements, the temperature field and vertical wind field are related with TWH, which represents the strong convection and release of latent heat of the hurricane. Thus TWH is effective for diagnosing the characteristics of the weather system.

From Eq. (46), we deduce that H_{1r} is small. In order to clarify this conclusion, H_{1r} and H_{1t} are calculated separately by using Eqs. (45) and (46). Figure 4 gives the calculated values. Figures 4a and 4c are the distributions of H_{1t} and H_{1r} at 400 hPa. Figures 4b and 4d show the vertical cross sections of H_{1t} and H_{1r} along the heavy line in Fig. 4a. The scale of the H_{1r} is $O(10^{-5}\ \mathrm{s}^{-2})$, and that of the H_{1t} is $O(10^{-4}\ \mathrm{s}^{-2})$. Thus, the TWH mainly depends on its tangential component.

Equation (11) is used to calculate the SWH in Hurricane Andrew (Fig. 5). Figure 5a is the horizontal component at 400 hPa and Fig. 5b is the vertical cross section along the heavy line in Fig. 5a. A comparison of Fig. 3a and Fig. 5a shows that the region of TWH is much larger than that of SWH, however the maximum value of SWH is larger than that of TWH. It is found that there is no value in the low level in Fig. 3b, which is different from Fig. 5b. This is accounted for by the divergence term showing the strong vertical vorticity and convergence in the low level; however TWH presents strong convection and release of latent heat in the middle-upper level. The characteristics of H_1 and H_2 are clearly presented in Fig. 4 through SWH.

5. Application of SWH in studying the development of Hurricane Andrew

Equation (22) implies that the SWH is closely related with the individual change of vorticity and has the potential ability to forecast. In this section, the SWH is applied to study the development of Hurricane Andrew (1992) to validate its practicability.

The horizontal component of the variation of vorticity at 400 hPa is presented in Fig. 6, showing the vorticity at 1200 UTC 23 August 1992 minus the vorticity at 0600 UTC 23 August 1992. The left region of Fig. 6 is similar with the same place in Fig. 4a, which is the SWH at 0900 UTC 23 August 1992. Figure 6 just shows the variation at a single point in time, and the variation of the temporal series will be shown later. The center of circulation for Hurricane Andrew was defined by a local maximum of relative vorticity at 900 hPa averaged over a 360 km×360 km square (Davis and Bosart, 2003). $\overline{\zeta}$ and $\overline{H}_s$, using Eqs. (20) and (21), are calculated in the region for the vertical levels from 1000 hPa to 200 hPa. The central difference method is used to calculate $\partial\overline{\zeta}/\partial t$. The variations of $\partial\overline{\zeta}/\partial t$ and $\overline{H}_s$ with respect to time are presented in Fig. 7, in which the values have been normalized. It is evident from the figure that the tendency of the average vorticity and the average SWH have the same trend with respect to time, which indicates that the SWH is an effective variable for diagnosing the development of

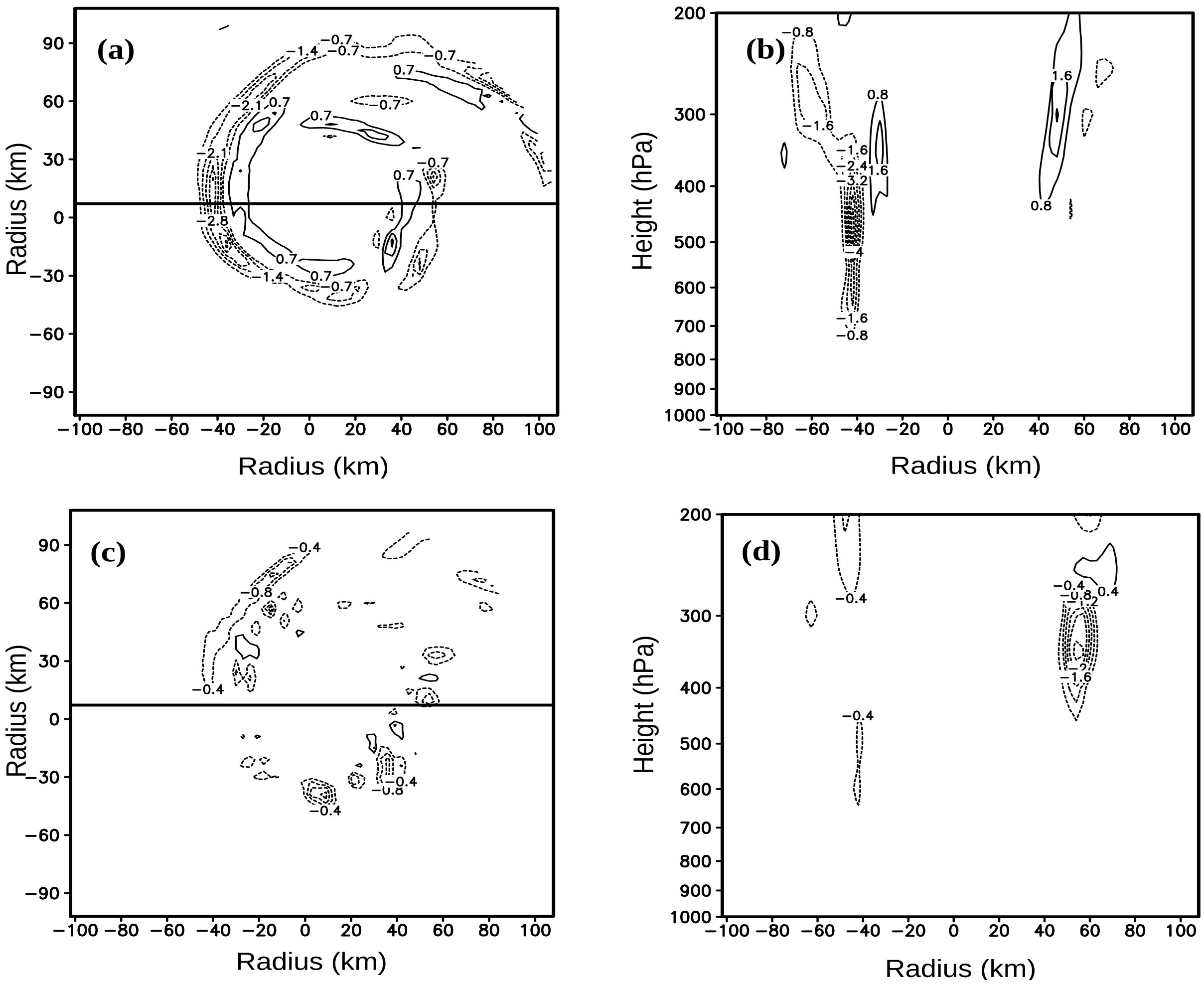

Fig. 4. H_{1t} ($0.0001\,s^{-2}$) and H_{1r} ($0.0001\,s^{-2}$) calculated by Eqs. (25) and (24). (a) Tangential component H_{1t} at 400 hPa, (b) Vertical cross section of H_{1t} along the heavy line in (a), (c) Radial component H_{1r} at 400 hPa, (d) Vertical cross section of H_{1r} along the heavy line in (c).

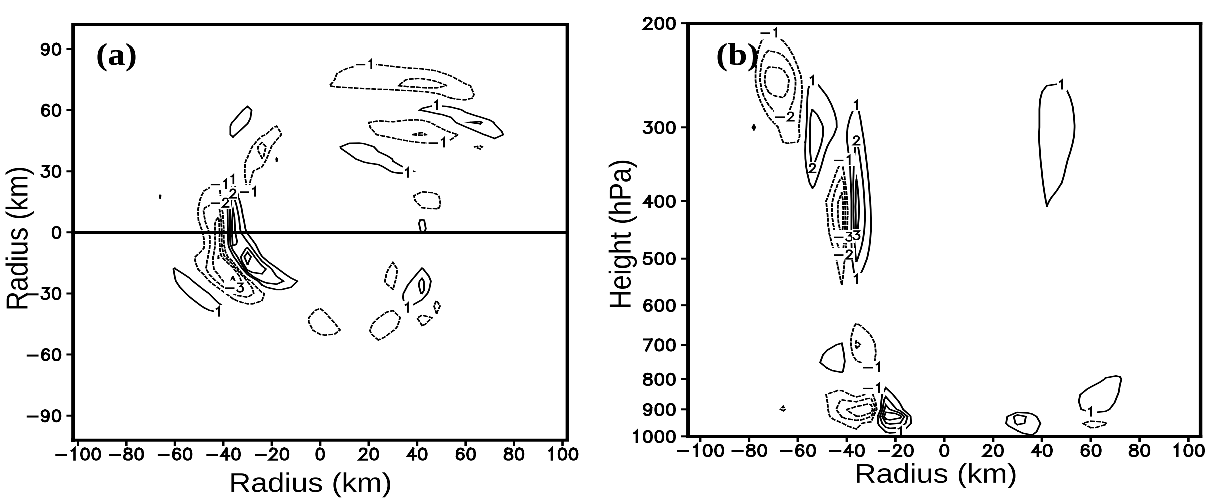

Fig. 5. SWH ($0.0001\,s^{-2}$) of Hurricane Andrew at 0900 UTC 23 August 1992. (a) SWH at 400 hPa. (b) Vertical cross section of SWH along the heavy line in (a).

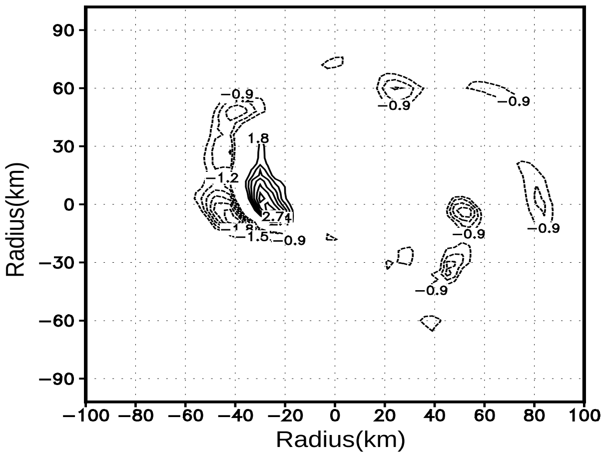

Fig. 6. Variation of vorticity ($0.001\,\mathrm{s}^{-1}$) at 400 hPa, showing the vorticity at 1200 UTC 23 August 1992 minus that at 0600 UTC 23 August 1992.

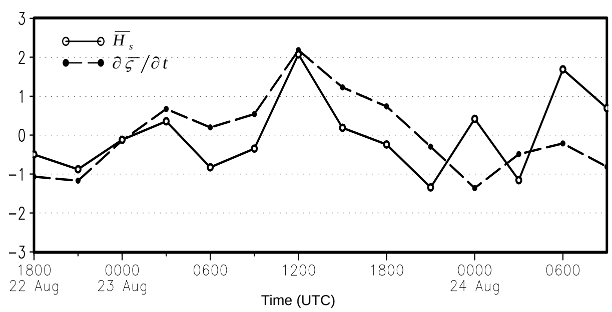

Fig. 7. The variation of $\partial\overline{\zeta}/\partial t$ (dashed) and $\overline{H}_s$ (solid) with respect to time.

the hurricane. From this example, it is apparent that the SWH may be one of the useful physical variables in a diagnosis analysis. In addition, it is also found that the two curves do not coincide with each other exactly in Fig. 7, especially at 0000 UTC and 0300 UTC 24 August 1992. Since there are only fourteen points, the linear correlation coefficient between $\partial\overline{\zeta}/\partial t$ and $\overline{H}_s$ is 0.42413. This may be ascribed to the neglect of the friction and solenoid terms in Eq. (22) which play an important role at that time.

6. Concluding remarks

Helicity has been extensively used to study the properties of weather systems such as tornadoes, squall lines and some other severe weather systems since the 1980s. Since helicity, by definition, is the scalar product of the velocity and vorticity vectors, it may be positive or negative according to the features of these vectors (Maffatt, 1969, 1978, 1981). For example, if the cyclonic rotation of the flow is combined with upward vertical motion, the helicity is positive, while with downward motion, it is negative. The direct relationship of the helicity to a weather system is not quite clear or obvious. However, as we generalize the concept of helicity as SWH, $H_s = \boldsymbol{\omega}_a \cdot (\partial \boldsymbol{V}/\partial z)$, then the situation will change. The relationship of the SWH with the vorticity of a weather system becomes clearer. It is found that the volume-averaged SWH depicts the variation of cyclonic rotation of the weather system dynamically. TWH is generalized if the geostrophic assumption is used, which depicts the strength of rotation in the direction of the thermal wind. The characteristics of TWH and SWH are studied by calculating the MM5 model output of a successfully-simulated hurricane. TWH, which represents the strong convection and release of latent heat in the middle-upper layer of a hurricane, is effective for diagnosing the features of a weather system. SWH, including the TWH and divergence term, is effective for diagnosing the development of a hurricane. Although the findings reported herein are based on a sole case study and thus cannot yet be generalized, it is believed that the SWH and TWH are sufficiently interesting to warrant their further testing in the research of tropical cyclone genesis.

APPENDIX

Helicity for Shallow Water

The governing equations for shallow-water motion are

$$\frac{du}{dt} - fv = -g\frac{\partial h}{\partial x} \tag{A1}$$

$$\frac{dv}{dt} + fu = -g\frac{\partial h}{\partial y} \tag{A2}$$

$$\frac{dh}{dt} + h\left(\frac{\partial u}{\partial x} + \frac{\partial v}{\partial y}\right) = 0\,, \tag{A3}$$

where

$$\frac{d}{dt} = \frac{\partial}{\partial t} + u\frac{\partial}{\partial x} + v\frac{\partial}{\partial y}$$

and h is the height of the water surface. From Eqs. (A1) and (A2), we can obtain the vorticity equation as follows:

$$\frac{d}{dt}(\zeta + f) = -(\zeta + f)\left(\frac{\partial u}{\partial x} + \frac{\partial v}{\partial y}\right)\,. \tag{A4}$$

Since the kinetic boundary condition at the water surface $z = h(x, y)$ is

$$w = \frac{dh}{dt}\,, \tag{A5}$$

and with the definition of helicity, we have

$$H = (\zeta + f)w = (\zeta + f)\frac{dh}{dt}\,. \tag{A6}$$

For the large-scale atmospheric motion, $(\zeta + f)$ is generally greater than zero, thus, the sign of H is dependent on the vertical motion. For the upward motion, $H > 0$, while for the downward motion, $H < 0$.

With Eqs. (A3) and (A4), (A6) can be rewritten as

$$\begin{aligned} H &= (\zeta + f)\frac{dh}{dt} \\ &= -h(\zeta + f)\left(\frac{\partial u}{\partial x} + \frac{\partial v}{\partial y}\right) \\ &= h\frac{d}{dt}(\zeta + f)\,, \end{aligned} \tag{A7}$$

which indicates that, for upward (downward) motion, H is positive (negative) and correspondingly, the vorticity will increase (decrease). Equation (A7) shows that, in the framework of the shallow-water model, the helicity is closely related with the tendency of vorticity. However, such a relation cannot be found for general three-dimensional motions.

Acknowledgments. This work was supported by the National Natural Science Foundation of China (Grant Nos. 40475024 and 40333025), and the foundation for Ph.D specialty of the Ministry of Education (Grant No. 20020284016). The authors would like to thank Prof. Dalin Zhang for his generosity in providing the model output data and Dr. Yangang Lui of Brookhaven National Laboratory for his valuable suggestions.

REFERENCES

Brown, R. A., 1980: Longitudinal instabilities and secondary flows in the planetary boundary layer: A review. *Rev. Geophys. Space Phys.*, **18**, 683–697.

Chen Hua, and Tan Zhemin, 1999: Helicity dynamics in a tropical cyclone. *Journal of Tropical Meteorology*, **15**, 81–85. (in Chinese)

Davis, C. A., and L. E. Bosart, 2003: Baroclinically induced tropical cyclogesis. *Mon. Wea. Rev.*, **131**, 2730–2746.

Etling, D., 1985: Some aspects of helicity in atmospheric flows. *Beitr. Phys. Atmos.*, **58**, 88–100.

Holton, J. R., 2004: *An Introduction to Dynamic Meteorology.* Elsevier Academic Press, 104pp.

Hoskins, B. J., M. E. McIntyre, and A. W. Robertson, 1985: On the use and significance of isentropic potential vorticity maps. *Quart. J. Roy. Meteor. Soc.*, **111**, 877–946.

Lilly, D. K., 1986: The structure, energetics and propagation of rotating convective storms. Part II: Helicity and storm stabilization. *J. Atmos. Sci.*, **43**, 126–140.

Lilly, D. K., 1990: Numerical prediction of thunderstorms—Has its time come? *Quart. J. Roy. Meteor. Soc.*, **116**, 779–798.

Liu, Y., D.-L. Zhang, and M. K. Yau, 1997: A multiscale numerical study of Hurricane Andrew (1992). Part I: Explicit simulation and verification. *Mon. Wea. Rev.*, **125**, 3073–3093.

Liu, Y., D.-L. Zhang, and M. K. Yau, 1999: A multiscale numerical study of Hurricane Andrew (1992). Part II: Kinematics and inner core structures. *Mon. Wea. Rev.*, **147**, 2597–2616.

Maffatt, H. K., 1969: The degree of knottedness of tangled vortex lines. *J. Fluid Mech.*, **35**, 117–129.

Maffatt, H. K., 1978: *Magnetic Field Generation in Electrically Conducting Fluids.* Cambridge University Press, 122pp.

Maffatt, H. K., 1981: Some developments in the theory of turbulence. *J. Fluid Mech.*, **35**, 27–49.

Tan Zhemin, and Wu Rongsheng, 1994: Helicity dynamics of atmospheric flow. *Adv. Atmos. Sci.*, **11**, 175–188.

Wu Rongsheng, 1984: On the change of enstrophy in the atmosphere. *Chinese Science Bulletin*, **24**, 1384–1386. (in Chinese)

Wu Rongsheng, and Tan Zhemin, 1989: Conservation laws on generalized vorticity and potential vorticity and its application. *Acta Meteorologica Sinica*, **47**, 436–442. (in Chinese)

Xu Yamei, and Wu Rongsheng, 2003: The conservation of helicity in hurricane Andrew (1992) and the formation of the spiral rainband. *Adv. Atmos. Sci.*, **20**, 940–950

Zhang, D.-L., Y. Liu, and M. K. Yau, 2000: A multiscale numerical study of Hurricane Andrew (1992). Part III: Dynamically-induced vertical motion. *Mon. Wea. Rev.*, **128**, 3722–3788.

Zhang, D.-L., Y. Liu, and M. K. Yau, 2004: A multiscale numerical study of Hurricane Andrew (1992). Part IV: Unbalanced flows. *Mon. Wea. Rev.*, **132**, 1410–1433.